Exploring topological phases with quantum walks

Takuya Kitagawa, Mark S. Rudner, Erez Berg, and Eugene Demler
Department of Physics, Harvard University, Cambridge, Massachusetts 02138, USA
(Received 23 July 2010; published 24 September 2010)

The quantum walk was originally proposed as a quantum-mechanical analog of the classical random walk, and has since become a powerful tool in quantum information science. In this paper, we show that discrete-time quantum walks provide a versatile platform for studying topological phases, which are currently the subject of intense theoretical and experimental investigations. In particular, we demonstrate that recent experimental realizations of quantum walks with cold atoms, photons, and ions simulate a nontrivial one-dimensional topological phase. With simple modifications, the quantum walk can be engineered to realize all of the topological phases, which have been classified in one and two dimensions. We further discuss the existence of robust edge modes at phase boundaries, which provide experimental signatures for the nontrivial topological character of the system.

DOI: 10.1103/PhysRevA.82.033429 PACS number(s): 37.10.Jk, 05.30.Rt, 42.50.−p

I. INTRODUCTION

Quantum walks, the quantum analogs of classical random walks [1], form the basis of efficient quantum algorithms [2,3], and provide a universal platform for quantum computation [4]. Much like their classical counterparts, quantum walks can be used to model a wide variety of physical processes including photosynthesis [5,6], quantum diffusion [7], optical or spin pumping and vortex transport [8], and electrical breakdown [9,10]. Motivated by the prospect of such an array of applications, several groups have recently realized quantum walks in experiments using ultracold atoms in optical lattices [11], trapped ions [12,13], photons [14,15], and nuclear magnetic resonance [16]. These systems offer the possibility to study quantum dynamics of single or many particles in a precisely controlled experimental setting.

Here, we show that quantum walks can be used to explore dynamics in a wide range of topological phases [17–19]. Interest in topological phases was first sparked by the discovery of the integer-quantized Hall (IQH) effect [19,20], and has rapidly increased in recent years following the prediction [21–23] and experimental realization [24,25] of a new class of materials called topological insulators. Unlike more familiar states of matter, such as the ferromagnetic and superconducting phases, which break SU(2) (spin-rotation) and U(1) (gauge) symmetries, respectively, topological phases do not break any symmetries and cannot be described by any local-order parameters. Rather, these phases are described by topological invariants, which characterize the global structures of their ground-state wave functions. Topological phases are known to host a variety of exotic phenomena, such as fractional charges and magnetic monopoles [26,27]. Motivated by such possibilities, there has been a great effort to realize and study topological phases in well-controlled systems composed of photons [28] or cold atoms and molecules [29–42].

In this paper, we investigate the realization of topological phases in discrete-time quantum walks (DTQWs). In a DTQW, a walker with a twofold internal spin degree of freedom is made to hop between adjacent sites of a lattice through a series of unitary operations [Fig. 1(a)]. As we explain subsequently, this discrete-time quantum dynamics can be described in terms of an effective band structure [see Fig. 1(b)] with strong spin-orbit coupling. We will show that the one-dimensional (1D) version of the DTQW, which was recently demonstrated in experiments [11,12,14,15] realizes a nontrivial 1D topological phase. This topological phase is analogous to that of the Su-Schrieffer-Heeger (SSH) model of polyacetylene [17]. The topology of this phase is characterized by a nonzero winding of the spinor eigenstates on a great circle of the Bloch sphere, as illustrated in Fig. 1(b). We discuss how, with slight modifications of the DTQW protocol, DTQWs can realize a wide range of topological phases in 1D and two dimensions (2D).

The class of topological phases, which can be realized in a system of noninteracting particles is determined by the dimensionality of the system and the underlying symmetries of its Hamiltonian. Figure 2 shows the ten classes of topological phases, which can arise in 1D and 2D systems with and without time-reversal symmetry (TRS) and particle-hole symmetry (PHS) (see Refs. [26,43,44] and discussion following). If both symmetries are absent in 1D, the possibility of a distinct chiral symmetry creates an additional class of topological phases. Within each class, the allowed phases are characterized by either an integer (Z) or a binary (Z_2) topological invariant. In DTQWs, both PHS and TRS can be realized by an appropriate choice of the DTQW protocol. While a single class of topological phase is typically realized in any particular condensed-matter system, we find that DTQWs can be used to simulate all of the phases listed in Fig. 2. Thus, DTQWs provide a powerful realizable platform that enables the experimental study of the entire periodic table of topological phases classified in Refs. [43,44] in 1D and 2D.

The nontrivial topological properties of the systems classified in Fig. 2 are manifested in the presence of robust edge states at phase boundaries (i.e., zero energy bound states [18] and gapless edge modes [45] in 1D and 2D systems, respectively). We propose a scheme to identify the presence of topological phases through the observation of edge modes at an interface between regions where different DTQW protocols are applied.

The prospect of creating topological phases in atomic or optical systems using DTQWs offers a unique opportunity to study dynamics in these phases using direct local probes of the

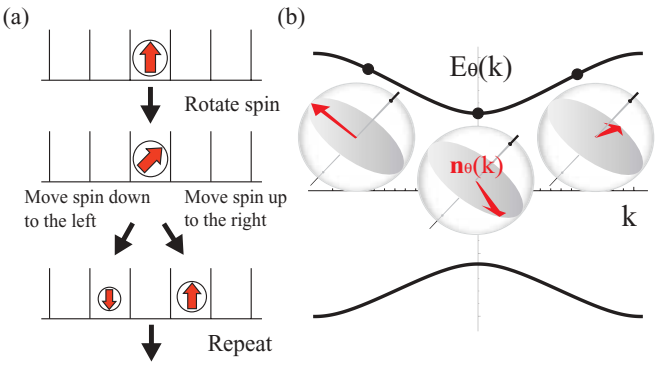

FIG. 1. (Color online) (a) One-dimensional DTQW protocol. First, the walker's internal spin is rotated through an angle θ about the y axis. Then, the walker is coherently translated by one lattice site to the right (left) if its spin is up (down), respectively. The quantum walk is produced by repeatedly applying this combined step operation. (b) Effective band structure of 1D DTQW with $\theta = \pi/2$. The spinor eigenstates at each momentum k are directed along the unit vector $\mathbf{n}_\theta(k)$ [see Eq. (6)], as represented on the Bloch sphere. $\mathbf{n}_\theta(k)$ always lies on a plane perpendicular to a constant vector $\mathbf{A}_\theta$ containing the origin (see text). Note that $\mathbf{n}_\theta(k)$ winds around the origin once as k traverses the Brillouin zone (BZ).

particle's wave function. Moreover, the unprecedented controllability of these systems opens the possibility for systematic investigations of quantum phase transitions between different topological phases, and of the robustness of these phases to a variety of perturbations including impurities, decoherence, interactions, and explicit breaking of symmetries.

II. TOPOLOGICAL PHASES IN 1D

The 1D DTQW protocol employed in recent experiments [11–16] is depicted schematically in Fig. 1(a). The basis states of the system are described in terms of the position of the walker, defined on integer lattice sites x, and its internal spin state, which can be either up ($\uparrow$) or down ($\downarrow$).

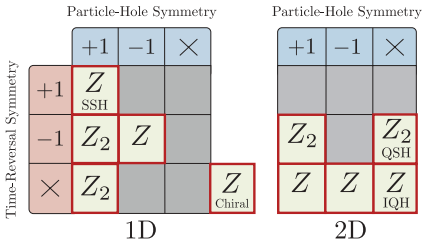

FIG. 2. (Color online) Topological phases realized by DTQWs. DTQWs can naturally realize all ten classes of nontrivial topological phases in 1D and 2D, see Refs. [43,44]. TRS and PHS are defined by the existence of antiunitary operators $\mathcal{T}$ and $\mathcal{P}$ satisfying Eqs. (7) and (8), and may be absent, or present with $\mathcal{T}^2 = \pm 1$ ($\mathcal{P}^2 = \pm 1$). In the absence of both TRS and PHS, a distinct chiral symmetry with a unitary Γ satisfying Eq. (9) may be found. In each case, the symmetry-allowed phases are classified by an integer (Z) or binary (Z_2) topological invariant. Classes containing the SSH model [17], IQH [19,20], and quantum spin Hall (QSH) [21–25] phases are indicated.

The quantum evolution is produced by repeatedly applying a unitary operation,

$$U(\theta) = T\,R(\theta), \tag{1}$$

that defines one step of the quantum walk. Each step consists of a spin rotation $R(\theta)$, followed by a coherent spin-dependent translation,

$$T = \sum_x [|x+1\rangle\langle x| \otimes |\uparrow\rangle\langle\uparrow| + |x-1\rangle\langle x| \otimes |\downarrow\rangle\langle\downarrow|], \tag{2}$$

that shifts the walker to the right (left) by one lattice site if its spin is up (down). This step protocol is a unitary generalization of the classical process in which a random walker hops left or right according to the outcome of a stochastic coin flip. Here, as in the experiments of Refs. [11–13], we consider the case where $R(\theta)$ corresponds to a spin rotation around the y axis through an angle θ,

$$R(\theta) = \begin{bmatrix} \cos(\theta/2) & -\sin(\theta/2) \\ \sin(\theta/2) & \cos(\theta/2) \end{bmatrix}. \tag{3}$$

Although the step protocol is defined explicitly in terms of the discrete unitary operations T and $R(\theta)$, the net evolution over one step is equivalent to that generated by a time-independent effective Hamiltonian $H(\theta)$ over the step time δt,

$$U(\theta) = e^{-iH(\theta)\,\delta t}, \quad \hbar = 1. \tag{4}$$

The evolution operator for N steps is given by $U^N(\theta) = e^{-iH(\theta)N\,\delta t}$. Thus, the DTQW provides a stroboscopic simulation of the evolution generated by $H(\theta)$ at the discrete times $N\,\delta t$. In the following, we take units in which $\delta t = 1$.

The DTQW protocol described earlier is translationally invariant. The evolution operator $U(\theta)$ and the Hamiltonian $H(\theta)$ are thus diagonalized down to 2×2 blocks in the basis of Fourier modes $|k\rangle \otimes |\sigma\rangle = \frac{1}{\sqrt{2\pi}} \sum_x e^{-ikx} |x\rangle \otimes |\sigma\rangle$, with $-\pi \leqslant k < \pi$. For the choice of $R(\theta)$ in Eq. (3), $H(\theta)$ can be written as

$$H(\theta) = \int_{-\pi}^{\pi} dk\, [E_\theta(k)\, \mathbf{n}_\theta(k) \cdot \sigma] \otimes |k\rangle\langle k|, \tag{5}$$

where $\sigma = (\sigma_x, \sigma_y, \sigma_z)$ is the vector of Pauli matrices and the unit vector $\mathbf{n}_\theta(k) = (n_x, n_y, n_z)$ defines the quantization axis for the spinor eigenstates at each momentum k. Because the evolution is prescribed stroboscopically at unit intervals, the eigenvalues $\pm E_\theta(k)$ of $H(\theta)$ are only determined up to integer multiples of 2π. The corresponding band structure is thus a quasienergy spectrum, with 2π periodicity in energy. For $\theta \neq 0$ or 2π, explicit expressions for $E_\theta(k)$ and $n_\theta(k)$ are given by $\cos E_\theta(k) = \cos(\theta/2) \cos k$ and

$$\mathbf{n}_\theta(k) = \frac{[\sin(\theta/2) \sin k,\ \sin(\theta/2) \cos k,\ -\cos(\theta/2) \sin k]}{\sin E_\theta(k)}. \tag{6}$$

A typical band structure $\pm E_\theta(k)$ is shown in Fig. 1(b). Note that for $\theta_* = 0$ or 2π, the spectrum of $H(\theta_*)$ is gapless, and $\mathbf{n}_{\theta_*}(k_*)$ is ill defined for $k_* = 0, \pi$.

Hamiltonians of the form (5) can support topological phases if they possess certain symmetries, as indicated in Fig. 2. The TRS and PHS of this table are defined by the existence of

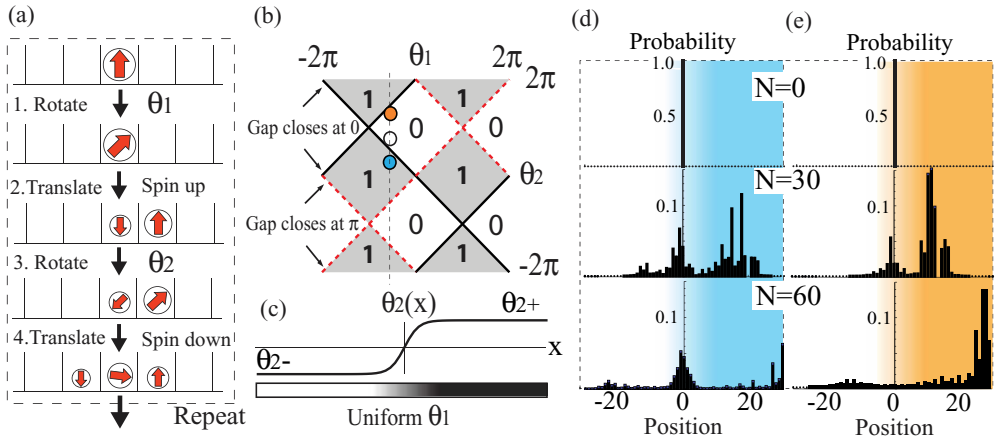

FIG. 3. (Color online) (a) One-dimensional split-step DTQW protocol, see Eq. (10). (b) Winding number associated with the split-step DTQW as a function of the spin-rotation angles θ_1 and θ_2. Topologically distinct gapped phases are separated by phase-transition lines where a gap closes at either $E = 0$ or $E = \pi$. (c) Phase boundary in the spatially inhomogeneous split-step DTQW. In the second rotation stage of Eq. (10), the walker's spin is rotated by an angle $\theta_2(x) = \frac{1}{2}(\theta_{2-} + \theta_{2+}) + \frac{1}{2}(\theta_{2+} - \theta_{2-}) \tanh(x/3)$. (d), (e) Dynamics of the spatially inhomogeneous split-step walk, with the walker initialized with spin up at $x = 0$. In both panels, we take $\theta_1 = -\pi/2$ and $\theta_{2-} = 3\pi/4$, corresponding to winding number 0 in the region $x \ll 0$ [white dot (middle) in panel b]. In (d), we create a phase boundary by taking $\theta_{2+} = \pi/4$, which gives winding number 1 for $x \gg 0$ [see blue dot (bottom) in panel b]. After many steps, the probability to find the walker near $x = 0$ remains large, indicating the existence of at least one localized state at the phase boundary. For this particular example, numerical diagonalization shows that there are three localized states at this boundary. In (e), we take $\theta_{2+} = 11\pi/8$ [orange (top) dot in panel b], so that the quantum walk in all regions is characterized by winding number 0. In this case, the probability to find the walker near $x = 0$ after many steps decays to 0, indicating the absence of a localized state at the boundary.

antiunitary operators $\mathcal{T}$ and $\mathcal{P}$ satisfying

$$\mathcal{T} H \mathcal{T}^{-1} = H, \tag{7}$$

$$\mathcal{P} H \mathcal{P}^{-1} = -H. \tag{8}$$

The Hamiltonian $H(\theta)$ given by Eqs. (5) and (6) possesses PHS ((8) with $\mathcal{P} \equiv K$, where K is the complex conjugation operator. To see this, note that the evolution operator $U(\theta)$ given by Eqs. (1)–(3) is real, and thus invariant under K. Along with Eq. (4), this implies $H^*(\theta) = -H(\theta)$, which satisfies Eq. (8) with $\mathcal{P} \equiv K$. In addition, using Eq. (6), it is straightforward to check that $H(\theta)$ possesses a unitary chiral symmetry of the form

$$\Gamma_\theta^{-1} H(\theta) \Gamma_\theta = -H(\theta), \tag{9}$$

with $\Gamma_\theta = e^{-i\pi \mathbf{A}_\theta \cdot \sigma/2}$, where $\mathbf{A}_\theta = [\cos(\theta/2), 0, \sin(\theta/2)]$ is perpendicular to $\mathbf{n}_\theta(k)$ for all k. The presence of both PHS (8) and chiral symmetry (9) guarantees that $H(\theta)$ is invariant under TRS (7) with $\mathcal{T} \equiv \Gamma_\theta \mathcal{P}$, see Refs. [43,44].

The symmetry classes identified in Fig. 2 are distinguished by whether the relevant symmetry operators $\mathcal{T}$ and $\mathcal{P}$ square to 1 or -1. Because here both $\mathcal{T}^2 = 1$ and $\mathcal{P}^2 = 1$, $H(\theta)$ belongs to the class of Hamiltonians labeled SSH. The corresponding integer-valued topological invariant Z has a simple geometrical interpretation. Chiral symmetry (9) constrains $\mathbf{n}_\theta(k)$ to lie on a plane, which is perpendicular to $\mathbf{A}_\theta$, and which contains the origin [see Fig. 1(b)]. Thus, $H(\theta)$ can be characterized by the number of times $\mathbf{n}_\theta(k)$ winds around the origin as k runs from $-\pi$ to π. Since the winding number of $\mathbf{n}_\theta(k)$ given by Eq. (6) is 1 for all $\theta \neq 0, 2\pi$, the DTQWs implemented in experiments [11–13] simulate the $Z = 1$ SSH topological phase.

The nontrivial topological character of the system can be revealed at a boundary between topologically distinct phases. To open the possibility to create such a boundary, we introduce the split-step DTQW protocol shown in Fig. 3(a). Starting from the DTQW defined by Eq. (1), we split the translations of the spin-up and spin-down components, and insert an additional spin rotation $R(\theta_2)$ around the y axis in between,

$$U_{\rm ss}(\theta_1, \theta_2) = T_\downarrow R(\theta_2) T_\uparrow R(\theta_1), \tag{10}$$

where $T_{\uparrow(\downarrow)}$ shifts the walker to the right (left) by one lattice site if its spin is up (down).

The split-step protocol defines a family of effective Hamiltonians $H_{\rm ss}(\theta_1, \theta_2)$ parametrized by the two spin-rotation angles θ_1 and θ_2. This family realizes both $Z = 0$ and $Z = 1$ SSH topological phases as displayed in Fig. 3(b), with chiral symmetry (9) given by $\Gamma_{\theta_1,\theta_2} \equiv \Gamma_{\theta_1}$, $\mathcal{P} = K$, and $\mathcal{T} = \Gamma_{\theta_1} \mathcal{P}$. We give the derivation of the phase diagram of Fig. 3(b) in Appendix A. Gapped phases with winding numbers $Z = 0$ and $Z = 1$ are separated by phase-transition lines where the quasienergy gap closes at either $E = 0$ or $E = \pm\pi$, as indicated in the figure.

We propose to create a phase boundary in the DTQW by replacing the second (spatially uniform) spin rotation $R(\theta_2)$ of Eq. (10) with a site-dependent spin rotation $R[\theta_2(x)]$, which rotates the walker's spin through an angle $\theta_2(x)$ about the y axis at each site x. Specifically, we consider the situation where $\theta_2(x) \to \theta_{2-}$ for $x \ll 0$ and changes monotonically to $\theta_2(x) \to \theta_{2+}$ for $x \gg 0$ [see Fig. 3(c)]. Although this protocol is not translationally invariant, symmetries (7)–(9) are preserved. In particular, the system retains the chiral symmetry under Γ_{θ_1} for arbitrary $\theta_2(x)$ as long as θ_1 remains uniform.

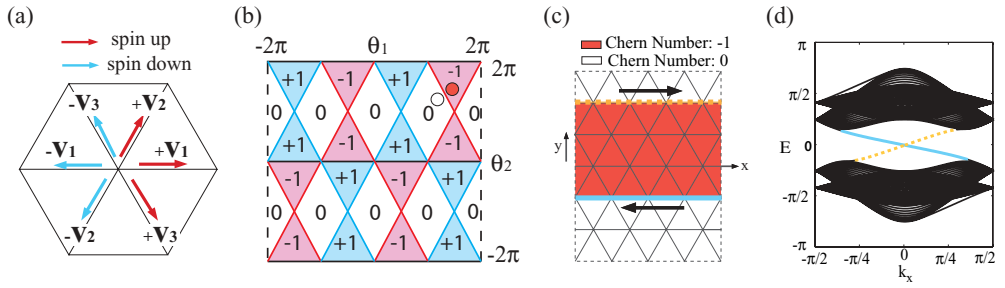

FIG. 4. (Color online) (a) Translation vectors for the triangular lattice 2D quantum walk defined in Eq. (11). (b) Chern number associated with the 2D DTQW as a function of the rotation angles θ_1 and θ_2. (c) Geometry of an inhomogeneous 2D quantum walk with periodic boundary conditions. In the red (middle) region, we take $\theta_1 = \theta_2 = 3\pi/2$, corresponding to Chern number -1, while in the white (top and bottom) regions, we take $\theta_1 = \theta_2 = 7\pi/6$, corresponding to Chern number 0 [see colored dot (upper) in panel (b)]. Arrows indicate the propagation directions of chiral edge modes localized at the two boundaries. (d) Quasienergy spectrum of the inhomogeneous 2D quantum walk depicted in panel (c) for a 100×100 site lattice. The BZ for momentum k_x parallel to the interface is defined for the doubled unit cell accessed by U_{2D}, Eq. (11). Two branches of chiral edge modes connect the upper and lower bands. The dotted (solid) line corresponds to the mode localized at the upper (lower) boundary in panel (c).

When the rotation angles (θ_1,θ_{2+}) and (θ_1,θ_{2-}) are chosen to realize topologically distinct phases with $Z = 0$ and $Z = 1$ in the regions $x \ll 0$ and $x \gg 0$, a bound state with energy 0 or π exists near the phase boundary $x = 0$ [18]. The existence of such a bound state is guaranteed by topology, and does not depend on the details of the boundary. The bound state can be probed by initializing the walker at $x = 0$ as demonstrated in Fig. 3(d). Because this initial state has a nonvanishing overlap with the bound state, part of the walker's wave packet will remain localized near $x = 0$. On the other hand, if the pairs (θ_1,θ_{2+}), (θ_1,θ_{2-}) are chosen to lie within the same diamond-shaped region of Fig. 3(b), then the system can be made spatially uniform through a continuous deformation of the Hamiltonian without closing either gap at $E = 0$ or $E = \pi$. In this case, there are no topologically protected modes localized at the boundary. For monotonic $\theta_2(x)$, this guarantees that the system does not support *any* bound states, and the probability to find the walker at $x = 0$ decays to zero with an increasing number of DTQW steps [see Fig. 3(e)]. The existence and absence of localized states at the boundary has been confirmed through numerical as well as analytical methods (See Appendix E).

With further modifications to the DTQW protocol, each of the topological classes in 1D given in Fig. 2 can be realized. The examples and detailed analysis of 1D quantum walk corresponding to each topological phase are described in Appendix B. In addition, as we will now discuss, a straightforward extension of the protocol to a higher-dimensional lattice allows the DTQW to simulate topological phases in 2D.

III. TOPOLOGICAL PHASES IN 2D

To begin, we consider a family of 2D quantum walks in which the walker possesses two internal states as in the previous 1D DTQWs. Nontrivial topological phases can be realized in a variety of 2D lattice geometries. Here, we consider the case of a triangular lattice, and discuss equivalent square lattice realizations in Appendix C. One step of the quantum walk is defined by the unitary operation,

$$U_{2D}(\theta_1,\theta_2) = T_3 R(\theta_1) T_2 R(\theta_2) T_1 R(\theta_1), \qquad (11)$$

where T_i $(i = 1,2,3)$ translates the walker with spin up (down) in the $+(-)\mathbf{v}_i$ direction, with $\{\mathbf{v}_i\}$ defined in Fig. 4(a). The net result of Eq. (11) is to make the walker hop between sites of a superlattice defined by twice the primitive unit cell. The effective Hamiltonian for this 2D DTQW takes the form of Eq. (5) with the integration over $\mathbf{k} = (k_x,k_y)$ taken over the 2D BZ of the superlattice.

We now study the topological properties of the 2D DTQWs defined by Eq. (11). The corresponding effective Hamiltonians lack TRS, and are thus contained in the symmetry classes in the bottom row of Fig. 2. Because U_{2D} is real, this system possesses PHS with $\mathcal{P} = K$ (see before). With a slight modification, this symmetry can be broken, and phases in the class labeled IQH in Fig. 2 can also be realized (see Appendix B). These phases are analogous to those of the Haldane model [46], which exhibits an IQH effect in the absence of a net magnetic field.

The phases realized by the 2D DTQW, Eq. (11), are characterized by an integer-valued topological invariant called the first Chern number. This quantity is defined in terms of the unit vector $\mathbf{n}(\mathbf{k})$, see Eq. (5), as $C = \frac{1}{4\pi}\int_{BZ} d^2k\,[\mathbf{n}\cdot(\partial_{k_x}\mathbf{n}\times\partial_{k_y}\mathbf{n})]$. Geometrically, the Chern number is equal to the number of times $\mathbf{n}(\mathbf{k})$ covers the unit sphere as $\mathbf{k}$ is taken over the 2D BZ. We have numerically calculated Chern numbers for 2D DTQWs throughout the full range of spin-rotation angles θ_1 and θ_2. We describe the details for the determination of the phase diagram for Fig. 4(b) in Appendix D. As shown in Fig. 4(b), phases with $C = 0$ and with $C = \pm 1$ can be realized.

Similar to the 1D case, nontrivial topology in 2D DTQWs is manifested in the presence of protected midgap modes bound to the interface between two topologically distinct phases. These gapless modes are analogous to the chiral edge modes of quantum Hall systems, and are robust against perturbations. To confirm the existence of such edge modes, we have used numerical diagonalization to study a nonuniform 2D DTQW on a 100×100 site triangular lattice with periodic boundary conditions, see Fig. 4(c). We take the spin-rotation angles θ_1 and θ_2 in Eq. (11) to be site dependent, with $\theta_1(y) = \theta_2(y) = 3\pi/2$ chosen to realize the $C = -1$ phase inside the red (middle) strip $25 \leqslant y < 75$, and $\theta_1(y) = \theta_2(y) = 7\pi/6$

chosen to realize the trivial $C = 0$ phase outside. The quasienergy spectrum is plotted in Fig. 4(d) as a function of the conserved momentum component k_x parallel to the interface. Two counterpropagating chiral edge modes exist inside the bulk gap. These modes are separately localized at the two boundaries between the $C = 0$ and $C = -1$ phases, as indicated in Fig. 4(c).

As described previously for 1D, these chiral edge modes can be probed by performing the spatially inhomogeneous 2D DTQW described earlier with the walker initialized at the boundary between two topologically distinct phases. Because a general state localized near the phase boundary has a nonzero overlap with the chiral edge mode, part of the walker's wave packet will propagate unidirectionally along the boundary. Such unidirectional propagation is protected by topology, and hence is robust even in the presence of an irregularly shaped boundary.

Finally,we present a time-reversal-invariant 2D DTQW with $\mathcal{T}^2 = -1$, which can realize the QSH phase (see Fig. 2). The realization of this phase requires the presence of at least four bands, which contain two pairs of time-reversed partners. Therefore, we now consider a DTQW where the walker possesses four internal states (e.g., a four-level atom, see also experiment [12]). We label these four states by a spin index σ, which takes the values $\uparrow$ and $\downarrow$, and a flavor index τ, which takes the values A and B. The time-reversal-invariant unitary step operator U_{TRI} is constructed in a block-diagonal form

$$U_{\mathrm{TRI}} = \begin{pmatrix} U_A & 0 \\ 0 & U_B \end{pmatrix}, \tag{12}$$

where U_A (U_B) only acts on the walker if its flavor index is equal to A (B). By fixing $U_B = U_A^T$, we ensure that U_{TRI} is invariant under the TRS operation $\mathcal{T} = i\tau_y K$, where τ_y is a Pauli matrix, which acts on the flavor index. As an example, if U_A is chosen according to Eq. (11), then $U_B = R(-\theta_1)T_1^T R(-\theta_2)T_2^T R(-\theta_1)T_3^T$. Note that T_i^T translates the walker in the direction $-(+)\mathbf{v}_i$ if its spin is up (down) (i.e., T_i^T) acts opposite to T_i.

Time-reversal invariant systems in 2D with $\mathcal{T}^2 = -1$ are characterized by a Z_2 topological invariant (middle row of right panel in Fig. 2). If θ_1 and θ_2 are chosen such that U_A is characterized by an odd Chern number, then U_{TRI} realizes a QSH phase with the Z_2 invariant equal to 1 [21]. Strictly speaking, the effective Hamiltonian corresponding to U_{TRI} conserves the flavor index τ and, as a result, supports topological phases classified by an integer Z, rather than the binary invariant Z_2. However, this additional symmetry can be broken by introducing a coupling between A and B states, which preserves TRS. In this way, the generic Z_2 classification can be retrieved. Explicit examples of 2D quantum walks corresponding to each topological phase in Fig. 2 are given in Appendix B.

IV. DISCUSSION AND SUMMARY

Because the edge modes bound to interfaces between topologically distinct phases in 1D and 2D are topologically protected, their existence is expected to be robust against a broad range of perturbations, which may arise in real experiments. In particular, their existence is insensitive to the details of the boundaries, which may be sharp or smooth, straight or curved (in 2D), etc. In some cases, the topological protection arises from certain symmetries (e.g., chiral symmetry in the 1D examples before). However, even if these symmetries are slightly broken by small errors in the spin-rotation axes and/or angles, the edge states are expected to persist due to the absence of nearby states inside the bulk energy gap.

Throughout this paper, we have focused on signatures of topological phases in single-particle dynamics. However, some dramatic manifestations of topological order (e.g., charge fractionalization and the quantization of the Hall conductivity) appear for specific many-body states such as the filled-band ground states of fermionic systems. To observe these phenomena in DTQWs with multiple walkers, analogous many-body states can be prepared schematically as follows. For special choices of the DTQW parameters, the Bloch eigenstates are simple (i.e., local in space, and uniform in spin). By preparing a single filled band comprised of such states, more complicated filled-band states can be obtained through a quasiadiabatic evolution in which the DTQW parameters are changed slightly from step to step. Even if an energy gap closes along the way, the number of excitations created in the process can be controlled by the effective sweep rate. In this way, many-body aspects of topological phases may also be studied using DTQWs.

In this paper, we have shown that DTQWs provide a unique setting in which to realize topological phases in 1D and 2D. With only slight modifications to the quantum walk protocol, which was realized in recent experiments, the entire periodic table of topological insulators [26,43,44] in 1D and 2D can be explored. In addition, we have provided a method to detect the presence of topological phases through the appearance of robust edge states at boundaries between topologically distinct phases.

Recently, several promising system-specific methods have been proposed to realize topological phases using cold atoms [29–41], polar molecules [42], or photons [28]. Our work advances this emerging field by providing a general framework for studying topological phases in a wide variety of available experimental systems including cold atoms, trapped ions, and photons. In the case of DTQWs, engineering of topological phases in DTQWs is enabled through the nonperturbative effect of dynamical drives.

By extending this work to three dimensions, it may be possible to realize new topological phases, such as the Hopf insulator [47], which have not yet been explored in condensed-matter systems. In addition, multiparticle generalizations of DTQWs will open new avenues in which to explore the quantum many-body dynamics of interacting fermionic or bosonic systems.

ACKNOWLEDGMENTS

We are grateful to Y. Shikano for introducing us to DTQWs. We thank M. D. Lukin and M. Levin for useful discussions. This work is supported by NSF Grant No. DMR 0705472, CUA, DARPA OLE, and AFOSR MURI. E.B. was also supported by the NSF under Grant No. DMR-0757145, and M.S.R. was supported by NSF Grants No. DMR 090647 and No. PHY 0646094.

APPENDIX A: DETERMINATION OF THE PHASE DIAGRAM FOR 1D SPLIT-STEP DTQW

The unitary evolution of the 1D split-step DTQW, Eq. (10), is generated by a Hamiltonian of the form of Eq. (5) with $\cos E(k) = \cos(\theta_2/2)\cos(\theta_1/2)\cos k - \sin(\theta_1/2)\sin(\theta_2/2)$, and

$$n_x(k) = \frac{\cos(\theta_2/2)\sin(\theta_1/2)\sin k}{\sin E(k)},$$
$$n_y(k) = \frac{\sin(\theta_2/2)\cos(\theta_1/2) + \cos(\theta_2/2)\sin(\theta_1/2)\cos k}{\sin E(k)},$$
$$n_z(k) = \frac{-\cos(\theta_2/2)\cos(\theta_1/2)\sin k}{\sin E(k)}. \quad \text{(A1)}$$

It is straightforward to check that $\mathbf{A}(\theta_1) = [\cos(\theta_1/2), 0, \sin(\theta_1/2)]$ is perpendicular to $\mathbf{n}(k)$ for all k. Therefore, the system possesses chiral symmetry (9) with $\Gamma(\theta_1) = e^{-i\pi\mathbf{A}(\theta_1)\cdot\sigma/2}$. As a result, the split-step DTQW can be characterized by the winding number of $\mathbf{n}(k)$ around the origin, denoted by Z. Using the explicit expression for $\mathbf{n}(k)$ in Eq. (A1), we find $Z = 1$ if $|\tan(\theta_2/2)/\tan(\theta_1/2)| < 1$, and $Z = 0$ if $|\tan(\theta_2/2)/\tan(\theta_1/2)| > 1$. The spectrum is gapless along the lines $|\tan(\theta_2/2)/\tan(\theta_1/2)| = 1$. Thus, we obtain the phase diagram displayed in Fig. 3(b).

APPENDIX B: EXPLICIT DTQW PROTOCOLS FOR ALL TOPOLOGICAL CLASSES

In this section, we provide explicit DTQW protocols, which can be used to realize topological phases in each of the symmetry classes listed in Fig. 2 of the main text. These protocols are summarized in Fig. 5. Each DTQW presented in Fig. 5 can realize both trivial and nontrivial phases within a given symmetry class. The specific phase, which is realized is determined by the spin-rotation angles, which parametrize the quantum walk; the system can be driven through a topological phase transition by tuning these spin-rotation angles. In the following, we denote the presence of TRS with $\mathcal{T}^2 = \pm 1$ by TRS $= \pm 1$, and the absence of TRS by TRS $= 0$. Similarly, we denote the presence of PHS with $\mathcal{P}^2 = \pm 1$ by PHS $= \pm 1$, and its absence by PHS $= 0$. We denote the presence of chiral symmetry under the unitary operator Γ by CH $= 1$, and its absence by CH $= 0$. Note that because the chiral symmetry operator Γ is *unitary*, rather than *antiunitary*, the phase of its square does not carry any additional information. In particular, the transformation $\Gamma \to e^{i\theta}\Gamma$ results in $\Gamma^2 \to e^{2i\theta}\Gamma^2$. For all of the DTQWs considered later, the presence of any two of the symmetries {TRS, PHS, CH} automatically ensures the presence of the third. For example, if a system possesses PHS and CH under the operators $\mathcal{P}$ and Γ, then it also possesses TRS under the operator $\mathcal{T} = \mathcal{P}\Gamma$.

1. Doubling procedure

Quantum walks with TRS $= -1$ can be readily constructed from DTQWs with TRS $= 0$ through the doubling procedure used to construct U_{TRI} [Eq. (12)] in the main text. First, the walker is endowed with an additional twofold flavor index τ, which can take either the value A or B. We then choose an evolution operator, which is diagonal in the flavor index and which satisfies $U_B = U_A^T$, where $U_{A(B)}$ is the evolution operator, which acts on the walker with flavor $A(B)$. With this possibility in mind, in the following, we focus on examples with TRS $= 0$.

2. One-dimensional topological phases

a. Symmetry classes: {TRS = 0, PHS = 0, CH = 1} (Z) {TRS = −1, PHS = −1, CH = 1} (Z)

The split-step DTQW described by Eq. (10) of the main text realizes the symmetry class with TRS $= 1$, PHS $= 1$, and CH $= 1$. By an appropriate change of the direction of the spin-rotation axes, TRS and PHS can be broken, while CH is retained. Thus, in order to realize the related symmetry classes

$\mathcal{T}^2$ (TRS)	$\mathcal{P}^2$ (PHS)	Γ^2 (CS)	1D DTQW protocol
1	1	1	$TR_y(\theta)$ or $T_\downarrow R_y(\theta_2)\,T_\uparrow R_y(\theta_1)$
—	—	1	$U_{\mathrm{ss}}^{\alpha} =$ $TR_\alpha(\theta)$ or $T_\downarrow R_\alpha(\theta_2)\,T_\uparrow R_\alpha(\theta_1)$
-1	-1	1	$\begin{pmatrix} U_{\mathrm{ss}}^{\alpha} & 0 \\ 0 & (U_{\mathrm{ss}}^{\alpha})^T \end{pmatrix}$
—	1	—	$U_{\mathrm{ss}'} = T_\downarrow R_y(\theta_2)\,T_\uparrow R_y(\theta_1)T$
-1	1	1	$\begin{pmatrix} U_{\mathrm{ss}'} & 0 \\ 0 & (U_{\mathrm{ss}'})^T \end{pmatrix}$

$\mathcal{T}^2$ (TRS)	$\mathcal{P}^2$ (PHS)	Γ^2 (CS)	2D DTQW protocol
—	—	—	$U_{\mathrm{2D}}^{\beta} = T_3 R_y(\theta_1) T_2 R_\beta(\theta_2) T_1 R_y(\theta_1)$
-1	—	—	$\begin{pmatrix} U_{2D}^{\beta} & 0 \\ 0 & 1 \end{pmatrix} e^{-i\tau_y\sigma_y\varphi/2} \begin{pmatrix} 1 & 0 \\ 0 & \left(U_{2D}^{\beta}\right)^T \end{pmatrix}$
—	-1	—	$\begin{pmatrix} U_{2D}^{\beta} & 0 \\ 0 & \left(U_{2D}^{\beta}\right)^* \end{pmatrix}$
—	1	—	$U_{\mathrm{2D}} = T_3 R_y(\theta_1) T_2 R_y(\theta_2) T_1 R_y(\theta_1)$
-1	1	1	$\begin{pmatrix} U_{2D} & 0 \\ 0 & (U_{2D})^T \end{pmatrix}$

FIG. 5. DTQW protocols for each symmetry class of topological phases in 1D and 2D. By tuning the rotation angles, all of these examples can realize both trivial and nontrivial topological phases within each class. Here, T translates the walker to the right (left) if its spin is up (down), while $T_\uparrow(T_\downarrow)$ translates only the spin-up (-down) component to the right (left). In 2D, the translation T_i shifts the walker in the $\mathbf{v}_i$ $(-\mathbf{v}_i)$ direction if its spin is up (down), see Fig. 4(a) of the main text. A spin-rotation operator $R_u(\theta)$ rotates the walker's spin through an angle θ about the axis $u \in \{y,\alpha,\beta\}$, where $\alpha = \frac{1}{\sqrt{2}}(0,1,1)$, and $\beta = [\sin(\pi/8), \cos(\pi/8), 0]$. In most cases, quantum walks with TRS $= -1$ and PHS $= -1$ are obtained by the doubling procedure starting from a quantum walk with evolution operator U_A, which has TRS $= 0$ and PHS $= 0$. Such cases are separated by dotted lines. See main text for descriptions of the relevant symmetry operators.

TRS $= 0$, PHS $= 0$, and CH $= 1$, we will break the PHS of the split-step DTQW.

In the main text, we showed that any DTQW whose unitary evolution operator is *real* possesses PHS with $\mathcal{P} = K$, where K is the complex-conjugation operator. The existence of PHS is in fact more general: If the two spin rotations in a split-step DTQW are performed around the same axis, and if that axis lies in the xy plane, then the DTQW will have PHS $= 1$. To see this, suppose that both rotations are performed around the axis $(\sin\varphi, \cos\varphi, 0)$. It is then straightforward to check that the resulting effective Hamiltonian possesses PHS under the operator $\mathcal{P} = e^{-i\sigma_z\varphi/2} K e^{i\sigma_z\varphi/2}$.

On the other hand, PHS is absent if we choose a rotation axis that contains a nonzero z component. An example of a DTQW with PHS $= 0$ is provided by the evolution operator,

$$U^{\alpha}_{\mathrm{ss}}(\theta_1,\theta_2) = T_{\downarrow} R_{\alpha}(\theta_2)\, T_{\uparrow} R_{\alpha}(\theta_1), \tag{B1}$$

where $R_\alpha(\theta)$ is a spin rotation around the axis $\alpha = \frac{1}{\sqrt{2}}(0,1,1)$ through the angle θ. Although PHS is absent, this system possesses chiral symmetry under the symmetry operator $\Gamma_\alpha(\theta_1) = ie^{-i\pi \mathbf{A}_\alpha(\theta_1)\cdot\sigma/2}$, where $\mathbf{A}_\alpha(\theta_1) = [\cos(\theta_1/2), \frac{1}{\sqrt{2}}\sin(\theta_1/2), \frac{1}{\sqrt{2}}\sin(\theta_1/2)]$. The absence of TRS can be checked in the following way. If the energy eigenvalues of the two states with momentum k are given by $\pm|E(k)|$, then TRS $= \pm 1$ requires $|E(k)| = |E(-k)|$. We have explicitly checked that this relation is not satisfied for the DTQW defined by Eq. (B1), and thus conclude that TRS is absent.

The preceding split-step DTQW, Eq. (B1), can realize distinct topological phases by tuning the spin-rotation angle θ_2. For example, the trivial phase with winding number $Z = 0$ is realized with $\theta_1 = \pi/2$ and $\theta_2 = 3\pi/4$, and the phase with winding number $Z = 1$ is realized with $\theta_1 = \pi/2$ and $\theta_2 = \pi/4$.

The recent experimental implementation of a DTQW with photons [14,15] employed the rotation operator given by the Hadamard gate $R_{\mathcal{H}} = ie^{-i\pi\mathbf{n}\cdot\sigma/2}$, with $\mathbf{n} = 1/\sqrt{2}(1,0,1)$. Since the rotation axis contains a nonzero z component, we conclude that this Hadamard walk belongs to the symmetry classes TRS $= 0$, PHS $= 0$, and CH $= 1$.

Using the doubling procedure described earlier, a TRS DTQW with TRS $= -1$, PHS $= -1$, and CH $= 1$ can be constructed based on the DTQW defined in Eq. (B1). The corresponding evolution for one step of the DTQW is given by $\mathrm{diag}\{U^{\alpha}_{\mathrm{ss}}(\theta_1,\theta_2), [U^{\alpha}_{\mathrm{ss}}(\theta_1,\theta_2)]^T\}$. It is straightforward to check that this quantum walk possesses chiral symmetry under the operator $\Gamma = \mathrm{diag}\,[\Gamma_\alpha(\theta_1), \Gamma^*_\alpha(\theta_1)]$. By construction, this DTQW possesses TRS $= -1$ with $\mathcal{T} = i\tau_y K$. Using these two symmetries, we construct a PHS operator $\mathcal{P} = \Gamma\mathcal{T}$ with $\mathcal{P}^2 = -1$.

b. Symmetry classes: {TRS = 0, PHS = 1, CH = 0} (Z_2) {TRS = −1, PHS = 1, CH = 1} (Z_2)

The construction of a DTQW with TRS $= 0$, PHS $= 1$, and CH $= 0$ starts from the split-step DTQW with TRS $= 1$, PHS $= 1$, and CH $= 1$ [see main text, Eq. (10)]. The chiral symmetry can be broken by adding extra operations to the split-step DTQW. On the other hand, in Sec. 2 *a*, we showed that PHS can be retained quite generally as long as the two rotation axes are the same and are taken to lie on the xy plane.

In order to construct a DTQW with CH $= 0$, we begin with Eq. (10) and add an additional spin-dependent translation T, which translates the walker to the right (left) by one lattice site if its spin is up (down) [see Eq. (2)]. Explicitly, the evolution operator for one step of a representative DTQW from this symmetry class is given by

$$U_{\mathrm{ss}'}(\theta_1,\theta_2) = T_{\downarrow} R_y(\theta_2)\, T_{\uparrow} R_y(\theta_1) T, \tag{B2}$$

where $R_y(\theta)$ is a spin rotation around the y axis through an angle θ [Eq. (3)]. Since $U_{\mathrm{ss}'}$ is real, this DTQW retains PHS $= 1$ with $\mathcal{P} = K$.

The absence of chiral symmetry for this walk can be verified by observing that the quantization axis $\mathbf{n}(k)$ does not lie on a plane, which includes the origin. Therefore, no single operator Γ can be found that satisfies $\Gamma H(k) = -H(k)\Gamma$ for all k.

One-dimensional systems with PHS exhibit two distinct topological phases [26]. These two phases are indexed by the Berry phase, which can only take the quantized values 0 and π due to the presence of PHS. Explicitly, the invariant is given by

$$B = \int \frac{dk}{2\pi}(-i)\langle\psi_{\mathrm{lb}}(k)|\partial_k|\psi_{\mathrm{lb}}(k)\rangle. \tag{B3}$$

Here, $|\psi_{\mathrm{lb}}(k)\rangle$ is the eigenstate in the lower band with momentum k. The DTQW described before can realize both topological phases, with the trivial phase ($B = 0$) realized for $\theta_1 = \pi/2, \theta_2 = \pi/6$, and the nontrivial phase with $B = 1/2$ realized for $\theta_1 = \pi/2, \theta_2 = 2\pi/3$.

Using the doubling procedure, we can construct a time-reversal invariant DTQW with TRS $= -1$, PHS $= 1$, and CH $= 1$ based on Eq. (B2).

3. Two-dimensional topological phases

a. Symmetry classes: {TRS = 0, PHS = 1, CH = 0} (Z) {TRS = −1, PHS = 1, CH = 1} (Z_2)

The triangular lattice 2D DTQW defined by Eq. (11) of the main text involves only spin rotations around the y axis. Consequently, the evolution operator U_{2D} is real and possesses PHS $= 1$ with $\mathcal{P} = K$. Therefore, the time-reversal invariant DTQW U_{TRI} constructed from U_{2D}, Eq. (12), is contained in the symmetry classes TRS $= -1$, PHS $= 1$, and CH $= 1$.

As noted in the main text, U_{TRI} is diagonal in the flavor index $\tau = A, B$ and thus possesses an extra symmetry related to the conservation of τ_z. Here, we describe a more general 2D DTQW with TRS $= -1$, which does not possess this additional symmetry. The operator for one step of this modified time-reversal invariant DTQW is given by

$$U_{\mathrm{TRI}'} = \begin{pmatrix} U_A & 0 \\ 0 & 1 \end{pmatrix} e^{-i\tau_y\sigma_y\varphi/2} \begin{pmatrix} 1 & 0 \\ 0 & U_B \end{pmatrix}, \tag{B4}$$

where U_A (U_B) acts on the walker if its flavor index is A (B). The rotation $e^{-i\tau_y\sigma_y\varphi/2}$ explicitly introduces mixing between the A and B flavors, and thus breaks the conservation of τ_z.

This DTQW is characterized by TRS $= -1$ with the symmetry operator $\mathcal{T} = i\tau_y K$ if U_B is chosen according to

$U_B = U_A^T$. If the Chern number associated with U_A is odd, then $U_{\mathrm{TRI}'}$ with $\varphi = 0$ realizes a nontrivial QSH topological phase. Because this phase is protected by TRS, the presence of a small $\varphi > 0$ cannot take the system out of this phase.

b. Symmetry classes: {TRS = 0, PHS = 0, CH = 0} (Z) {TRS = −1, PHS = 0, CH = 0} (Z_2)

The existence of topological phases characterized by a nonzero Chern number does not rely on the presence of PHS. Therefore, the topological phase with Chern number 1 in the TRS = 0, PHS = 1, and CS = 0 symmetry classes can be directly transformed to the corresponding phase in the TRS = 0, PHS = 0, and CS = 0 symmetry classes by a perturbation, which breaks PHS. Such a perturbation can be achieved by changing the rotation axis for the second rotation stage in Eq. (11). The resulting DTQW single-step evolution operator is given by

$$U_{2\mathrm{D}}^{\beta}(\theta_1,\theta_2) = T_3 R(\theta_1) T_2 R_\beta(\theta_2) T_1 R(\theta_1), \tag{B5}$$

where R is a spin rotation around the y axis, and $R_\beta(\theta)$ is a spin rotation around the axis $\beta = (\sin\varphi, \cos\varphi, 0)$ with $\varphi = \pi/8$. The operators $\{T_i\}$ correspond to spin-dependent translations along the directions $\{\mathbf{v}_i\}$, as defined in Fig. 4(a). The absence of PHS is confirmed by examining the relationship between energy eigenvalues $|E(\mathbf{k})|$ and $|E(-\mathbf{k})|$. The presence of PHS implies $|E(\mathbf{k})| = |E(-\mathbf{k})|$. This condition is violated for DTQW (B5). Therefore, this system does not possess PHS.

DTQW (B5) realizes both topologically trivial and nontrivial phases with zero and nonzero Chern numbers. For example, the choice $\theta_1 = \theta_2 = 3\pi/2$ generates the phase with Chern number -1, while $\theta_1 = \theta_2 = 7\pi/6$ corresponds to the phase with Chern number 0. Since PHS is absent, this DTQW belongs to the classes with TRS = 0, PHS = 0, and CS = 0. The related time-reversal invariant DTQW constructed by applying the doubling procedure to this walk has TRS = −1, PHS = 0, and CH = 0.

c. Symmetry classes: {TRS = 0, PHS = −1, CH = 0} (Z)

Quantum walks with PHS = −1 can be constructed through a doubling procedure similar to that used to construct DTQWs with TRS = −1. Consider the block-diagonal evolution operator,

$$U_{\mathrm{PHI}} = \begin{pmatrix} U_A & 0 \\ 0 & U_B \end{pmatrix}, \tag{B6}$$

where U_A (U_B) acts on the walker if its flavor index is A (B). If we choose $U_B = U_A^*$, then the resulting DTQWs possess PHS = −1 with $\mathcal{P} = i\tau_y K$. By choosing U_A according to Eq. (B5) with parameters to give a Chern number of 1, Eq. (B6) produces a DTQW, which realizes a nontrivial topological phase in the symmetry classes TRS = 0, PHS = −1, and CH = 0.

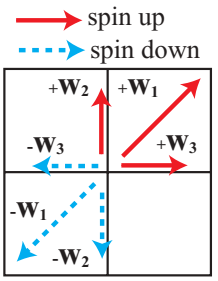

FIG. 6. (Color online) Translation vectors for 2D DTQW on a square lattice that realizes the phase diagram of Fig. 4 in the main text. Crucially, $\mathbf{v}_3$ satisfies the relation $\mathbf{v}_3 = \mathbf{v}_1 - \mathbf{v}_2$ just as in the triangular lattice realization.

APPENDIX C: REALIZATION OF 2D TOPOLOGICAL PHASES ON A SQUARE LATTICE

In the main text, we have provided examples of 2D DTQWs, which realize topological phases on a triangular lattice. However, these DTQWs can also be implemented on a square lattice, as we explain later. A square lattice may be easier to realize in some experimental implementations, such as cold atoms in optical lattices.

Generally speaking, the phase diagram of a DTQW is determined by the amplitude for the walker to hop from one site to another after one complete step of the evolution. Thus, as long as the hopping amplitudes between all pairs of sites are preserved, geometrical deformations of the lattice do not change the phase diagram. Therefore, the phase diagram of a DTQW is insensitive to geometric deformations of its host lattice.

In particular, 2D DTQWs with nonzero Chern numbers can be realized on a square lattice by replacing the translations along the vectors $\{\mathbf{v}_i\}$ on the triangular lattice in Eq. (11) with the vectors $\{\mathbf{w}_i\}$ shown in Fig. 6. Here, $\mathbf{w}_1 = (1,1)$, $\mathbf{w}_2 = (0,1)$, and $\mathbf{w}_3 = (1,0)$. This protocol is obtained simply by shearing the lattice used in Eq. (11) and Fig. 4(a). Note that the diagonal translation along $\mathbf{w}_1$ can be implemented by a compound translation along (1,0) followed by a translation along (0,1).

APPENDIX D: PHASE DIAGRAM OF THE 2D DTQW

Here, we briefly describe a general procedure for determining the phase diagrams of 2D DTQWs. Because the value of a quantized topological invariant can only change across a phase boundary where a gap closes, we first identify the lines in parameter space along which a gap vanishes in the quasienergy spectrum. Once these phase boundaries are determined, the topological phases between boundaries can be identified by computing the topological invariant at any single point within each region. For the 2D DTQW with an evolution operator given by Eq. (11), we have obtained phase boundaries analytically from the spectrum,

$$\begin{aligned}\cos E(\mathbf{k}) = \{&\cos(\theta_2/2)\cos\theta_1\cos[\mathbf{k}\cdot(\mathbf{v}_1+\mathbf{v}_2)] \\ &- \sin(\theta_2/2)\sin\theta_1\cos[\mathbf{k}\cdot(\mathbf{v}_1-\mathbf{v}_2)]\}\cos(\mathbf{v}_3\cdot\mathbf{k}) \\ &- \cos(\theta_2/2)\sin[\mathbf{k}\cdot(\mathbf{v}_1+\mathbf{v}_2)]\sin(\mathbf{v}_3\cdot\mathbf{k}),\end{aligned}$$

which gives the lines shown in Fig. 4(b). We then numerically evaluated the Chern number within each region using $C = \frac{1}{4\pi}\int_{\mathrm{BZ}} d^2k\,[\mathbf{n}\cdot(\partial_{k_x}\mathbf{n}\times\partial_{k_y}\mathbf{n})]$ with the appropriate expression for $\mathbf{n}(\mathbf{k})$.

APPENDIX E: LOCALIZED STATES AT A PHASE BOUNDARY OF INHOMOGENEOUS SPLIT-STEP 1D DTQW

In addition to the dynamical simulations presented in the main text, we have confirmed the existence of topologically protected edge states with energy $E = 0$ or $E = \pi$ in the 1D split-step DTQW through an analytical calculation for an infinite system with a *sharp* boundary, using $\theta_2(x) = \theta_{2-}$ for $x < 0$ and $\theta_2(x) = \theta_{2+}$ for $x \geqslant 0$. Furthermore, we have used numerical diagonalization to study the spectrum of a finite (periodic) system on a ring, which hosts two phase boundaries. In all cases, we find that, if the phases on the two sides of a boundary are topologically distinct (i.e., characterized by different winding numbers Z), then a single localized state with energy $E = 0$ or $E = \pi$ exists at the boundary.

For *smooth* boundaries as described in the main text, other localized states that are not protected by topology could appear. These bound states always appear in pairs with energies E and $-E$ due to chiral symmetry. Therefore, when the phases on the two sides of a boundary are topologically distinct, an odd number of bound states appears at the phase boundary [18].

[1] Y. Aharonov, L. Davidovich, and N. Zagury, Phys. Rev. A **48**, 1687 (1993).
[2] E. Farhi and S. Gutmann, Phys. Rev. A **58**, 915 (1998).
[3] N. Shenvi, J. Kempe, and K. Birgitta Whaley, Phys. Rev. A **67**, 052307 (2003).
[4] A. M. Childs, Phys. Rev. Lett. **102**, 180501 (2009).
[5] R. J. Sension, Nature (London) **446**, 740 (2007).
[6] M. Mohseni, P. Rebentrost, S. Lloyd, and A. Aspuru-Guzik, J. Chem. Phys. **129**, 174106 (2008).
[7] S. Godoy and S. Fujita, J. Chem. Phys. **97**, 5148 (1992).
[8] M. S. Rudner and L. S. Levitov, Phys. Rev. Lett. **102**, 065703 (2009).
[9] T. Oka, N. Konno, R. Arita, and H. Aoki, Phys. Rev. Lett. **94**, 100602 (2005).
[10] T. Oka and H. Aoki, Phys. Rev. Lett. **95**, 137601 (2005).
[11] M. Karski *et al.*, Science **325**, 174 (2009).
[12] F. Zähringer, G. Kirchmair, R. Gerritsma, E. Solano, R. Blatt, and C. F. Roos, Phys. Rev. Lett. **104**, 100503 (2010).
[13] H. Schmitz, R. Matjeschk, C. Schneider, J. Glueckert, M. Enderlein, T. Huber, and T. Schaetz, Phys. Rev. Lett. **103**, 090504 (2009).
[14] A. Schreiber, K. N. Cassemiro, V. Potoček, A. Gábris, P. J. Mosley, E. Andersson, I. Jex, and C. Silberhorn, Phys. Rev. Lett. **104**, 050502 (2010).
[15] M. A. Broome, A. Fedrizzi, B. P. Lanyon, I. Kassal, A. Aspuru-Guzik, and A. G. White, Phys. Rev. Lett. **104**, 153602 (2010).
[16] C. A. Ryan, M. Laforest, J. C. Boileau, and R. Laflamme, Phys. Rev. A **72**, 062317 (2005).
[17] W. P. Su, J. R. Schrieffer, and A. J. Heeger, Phys. Rev. Lett. **42**, 1698 (1979).
[18] S. Ryu and Y. Hatsugai, Phys. Rev. Lett. **89**, 077002 (2002).
[19] D. J. Thouless, M. Kohmoto, M. P. Nightingale, and M. den Nijs, Phys. Rev. Lett. **49**, 405 (1982).
[20] K. v. Klitzing, G. Dorda, and M. Pepper, Phys. Rev. Lett. **45**, 494 (1980).
[21] C. L. Kane and E. J. Mele, Phys. Rev. Lett. **95**, 146802 (2005).
[22] B. A. Bernevig, T. L. Hughes, and S.-C. Zhang, Science **314**, 1757 (2006).
[23] L. Fu and C. L. Kane, Phys. Rev. B **76**, 045302 (2007).
[24] M. Koenig *et al.*, Science **318**, 766 (2007).
[25] D. Hsieh *et al.*, Nature (London) **452**, 970 (2008).
[26] X.-L. Qi, T. L. Hughes, and S.-C. Zhang, Phys. Rev. B **78**, 195424 (2008).
[27] X.-L. Qi, T. L. Hughes, and S.-C. Zhang, Nat. Phys. **4**, 273 (2008).
[28] J. Otterbach, J. Ruseckas, R. G. Unanyan, G. Juzeliunas, and M. Fleischhauer, Phys. Rev. Lett. **104**, 033903 (2010).
[29] A. S. Sorensen, E. Demler, and M. D. Lukin, Phys. Rev. Lett. **94**, 086803 (2005).
[30] R. N. Palmer and D. Jaksch, Phys. Rev. Lett. **96**, 180407 (2006).
[31] T. D. Stanescu, C. Zhang, and V. M. Galitski, Phys. Rev. Lett. **99**, 110403 (2007).
[32] T. D. Stanescu, V. Galitski, J. Y. Vaishnav, C. W. Clark, and S. Das Sarma, Phys. Rev. A **79**, 053639 (2009).
[33] N. Goldman *et al.*, e-print arXiv:1002.0219.
[34] D. Jaksch and P. Zoller, New J. Phys. **5**, 56 (2003).
[35] E. J. Mueller, Phys. Rev. A **70**, 041603(R) (2004).
[36] I. B. Spielman, Phys. Rev. A **79**, 063613 (2009).
[37] F. Gerbier and J. Dalibard, New J. Phys. **12**, 033007 (2010).
[38] I. I. Satija, D. C. Dakin, J. Y. Vaishnav, and C. W. Clark, Phys. Rev. A **77**, 043410 (2008).
[39] S.-L. Zhu, H. Fu, C.-J. Wu, S.-C. Zhang, and L.-M. Duan, Phys. Rev. Lett. **97**, 240401 (2006).
[40] N. Goldman, A. Kubasiak, A. Bermudez, P. Gaspard, M. Lewenstein, and M. A. Martin-Delgado, Phys. Rev. Lett. **103**, 035301 (2009).
[41] K. Osterloh, M. Baig, L. Santos, P. Zoller, and M. Lewenstein, Phys. Rev. Lett. **95**, 010403 (2005).
[42] A. Micheli, G. K. Brenner, and P. Zoller, Nat. Phys. **2**, 341 (2006).
[43] A. P. Schnyder, S. Ryu, A. Furusaki, and A. W. W. Ludwig, Phys. Rev. B **78**, 195125 (2008).
[44] A. Kitaev, AIP Conf. Proc. **1134**, 22 (2009).
[45] B. I. Halperin, Phys. Rev. B **25**, 2185 (1982).
[46] F. D. M. Haldane, Phys. Rev. Lett. **61**, 2015 (1988).
[47] J. E. Moore, Y. Ran, and X.-G. Wen, Phys. Rev. Lett. **101**, 186805 (2008).